AXIAL COMPRESSION BEHAVIOR IN BRICK MASONRY WALLS: A COMBINED EXPERIMENTAL AND ANALYTICAL STUDY

Muhammad Zohaib Asim[1], Adnan Nawaz[2], Tahir Mehmood[3], Ali Siddique[4], Sajid Rasheed[5] and Asim Sultan[6]

[1,4,5,6]Lecturer, Civil Engineering Department, NUTECH, Islamabad 44000, Pakistan,

[1]muhammad.zohaib@nutech.edu.pk, [4]alisiddique@nutech.edu.pk,

[5]sajidrasheed@nutech.edu.pk, [6]asim.sultan@nutech.edu.pk

[2]Chairman, Civil Engineering Department, COMSATS University Islamabad, Wah Campus, Wah Cantt 47040, Pakistan, Pakistanadnannawaz@ciitwah.edu.pk

[3]Director QEC, Civil Engineering Department, COMSATS University Islamabad, Wah Campus, Wah Cantt 47040, Pakistan, drtahir.mehmood@ciitwah.edu.pk

ABSTRACT

In construction most of the buildings are constructed using brick as a load carry element while there are no standard guidelines and references to practice during preparation of bricks. There is no documented performance sheet available for the mechanical properties of bricks. In this study, bricks using different type of soil as per geological map of Pakistan manufactured by the conventional and zigzag technology are investigated for their mechanical properties. For the comparative analysis of the mechanical properties for the said brick types, 15 masonry prisms along with 10 masonry walls are constructed and investigated for the axial compression. Digital image correlation (DIC) is used to cross-validate the results of deformations measured with linear variable displacement transducer (LVDTs). Furthermore, software models using Abacus are used to correlate the damage analytically. It was observed that zig-zag bricks have more compressive strength than all other conventional bricks although bricks manufactured in Peshawar performed better than other counterparts. The results of this study can be used for designing the experimental program and effective decision-making techniques for mechanical properties of bricks in midrise masonry structure.

KEYWORDS: Digital Image Correlation, Analytical Model, Axial Compression, Masonry Structures, Height to Thickness Ratio

1. Introduction

Bricks have been widely used as building components used for masonry construction globally. Fired clay bricks are used to make load bearing walls in buildings [1]. It's reported that 1.3 trillion bricks are produced worldwide annually. Clay bricks are generally manufactured by baking clay molded blocks in brick kilns. Pakistan has a potential of producing 1.5% clay bricks of the total demand meet by twenty thousand Killens near the urban areas [2].

According to the geological map, Pakistan has a diverse distribution of the sedimentary and metamorphic which is ranging from mudstone to sandstone and shale. Zhang [3] and Oti et al [4] reported that a variation of clay content causes a change in the mechanical properties of bricks. Different tests were performed by researchers to investigate the mechanical properties of bricks. Toure et al [5] investigated the thermal capacity, thermal conductivity, and compressive strength of five different manufacturer bricks and concluded that the vibrated bricks exhibited a lower compressive strength of about 1.6 MPa as compared to an average compressive strength of 2.3 MPa in the case of compressed bricks. Dondi et al [6] investigated the mechanical properties and microstructure of the fired clay bricks and determined that for bricks with equal water absorption, fast firing tends to higher bond strength, lower bulk density, improved frost resistance, and greater mean pore size.

Masonry prisms offer a more accurate representation of actual construction, encapsulating the combined effects of masonry ingredients and workmanship quality. In a study by Singh and Munjal [7], 120 prisms made from burnt clay bricks and concrete blocks, using various mortar types, revealed that compressive strength increased with higher mortar strength and brick strength. Chen et al [8] further explored compressive strength assessment with 192 prisms using burnt clay and pressed-earth bricks, varying mortar proportions and h/t ratios. Their findings contribute to valuable insights into the performance of masonry elements.

Joyklad and Hussain [9] explored the axial and diagonal compressive behavior of ten masonry walls constructed with hollow interlocking bricks. Varying cement-sand grouts, with or without steel bars, revealed that walls with cement-sand grout exhibited reduced deformation. Employing advanced techniques like Zig-zag technology can lead to a 30% reduction in fuel consumption, enhancing heat distribution in the kiln and increasing the production of 1st class bricks from 60% to 95% [10,11]. Yooprasertchai et al [12] investigated

the mechanical properties of concrete made with recycled brick and concrete as a partial replacement for coarse aggregates which show less strength and stiffness than those made with natural aggregates. A cost-effective method using inexpensive glass fiber-reinforced polymer composites (LOC-GFRP) is proposed to address this. The ultimate strain and compressive strength were enhanced by 478% and 271%, respectively. With more LOC-GFRP layers, the resulting bilinear compressive stress vs. strain response demonstrated enhanced ductility and strength. Ali et al [13] investigated the use of plastic as a partial replacement for natural coarse particles in concrete. In order to achieve this, seven concrete mixes were produced by substituting natural aggregates with and without silica fume of comparable replacement levels with cement utilizing 0, 10, 15, and 20% plastic coarse particles. The results showed that adding plastic particles to concrete increased its workability but had a detrimental impact on its mechanical properties and fresh density. Without silica fume, plastic aggregate concrete's compressive and tensile strengths decreased by 32 and 33 percent, respectively.

2. Experimental program

Based on geology, Pakistan is widely distributed in many different classes of soil. According to the soil map of Pakistan, around 26 different types of soil exist in Pakistan. Based on the major soil types, five different regions were selected for the collection of 1st class bricks, as shown in Table 1.

The mechanical and physical properties of 1st class burnt clay bricks, collected from specified regions, were determined by absorption, compressive strength, modulus of rupture, and splitting tensile strength, according to ASTM standards. The typical dimension of the bricks used in this experimental program was L=9” W=4.5” H=3”. Before the construction of masonry prisms, the mechanical properties of mortar were determined by preparing 50mm mortar cubes, using one part of cement to 2.75 part of sand by weight with a w/c ratio of 0.485. Ordinary Portland Cement (OPC) was used with the highest compressive strength of 10,000 psi. Locally available sand was used to prepare mortar. 6 mortar specimens were prepared and tested under compression loading after 28 days. The test results of individual bricks and mortar are presented in Table 2. A total of 15 brick masonry prism specimens of varying h/t ratio i.e., 1.42, 2.17, and 2.93 using stack bond were constructed and tested

under compression using a Universal Testing Machine (UTM) with a capacity of 2000 KN. The tests were performed according to ASTM C1314-23a [14].

The thickness of the mortar joints in the masonry prism specimens was 10 mm. Steel plates were placed at the top and bottom of the specimens to ensure that the load was applied uniformly to the prism specimens. The load was applied uniformly not less than two or more than four minutes until the specimen collapsed. A total of 10 walls, single brick wall and double brick wall for each type given in Table 1, were constructed. An experienced mason was hired for the construction of walls. The thickness of the mortar joints was 10 mm. The dimensions of the wall specimens were 700 mm × 700 mm. The wall specimens were subjected to 28 days of curing. Hessian cloth technique was employed for curing wall specimens. The masonry walls were tested under pure axial compression as per ASTM C1717-18 [15] under a reaction frame with a capacity of 1000KN.

The axial load was applied using a hydraulic jack with a uniform rate until the wall failed. The propagation and intimation of cracks were visually inspected and recorded by a camera. A steel girder was used to distribute the load on the wall specimens. The experimental setup is illustrated in Fig. 1. One linear variable differential transducer (LVDT) was attached to the face of the walls to determine the axial deformation in mm that was noted using a data logger, as shown in Fig 2.

Table 1 Regional details

Regions	Type of soil	Brick type	Brick class	Cities
Region A	Alluvial soil	Conventional fired clay bricks	1st class	Peshawar
Region B	Loamy soil	Conventional fired clay bricks	1st class	Taxila
Region C	Calcareous sandy soil	Conventional fired clay bricks	1st class	Sargodha
Region D	Mainly loamy part gravelly soil	Conventional fired clay bricks	1st class	Quetta
Region E	Loamy and clayey soil	Zig-zag technology bricks	1st class (Zig-zag)	Rawalpindi

Table 2 Properties of constituent materials

Constituent material	Region	Test conducted	Test Result
Brick	Z	Absorption (%)	13.2
	P	ASTM C67-17 [16]	14.4
	S		16.2
	T		18.9
	Q		19.9
	Z	Compressive strength (MPa)	13.9
	P	ASTM C67-17 [16]	11.3
	S		9.8
	T		9.7
	Q		7.0
	Z	Modulus of rupture (MPa)	4.2
	P	ASTM C67-17 [16]	3.7
	S		2.8
	T		2.7
	Q		2.6
	Z	Splitting tensile strength (MPa)	1.3
	P	ASTM C1006-07 [17]	1
	S		0.7
	T		0.67
	Q		0.3
Mortar	Locally available sand	Compressive strength (MPa) ASTM C109/C109M-16a [18]	21.3

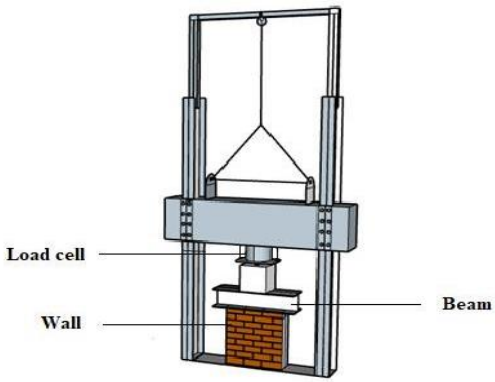

Figure 1 Experimental setup

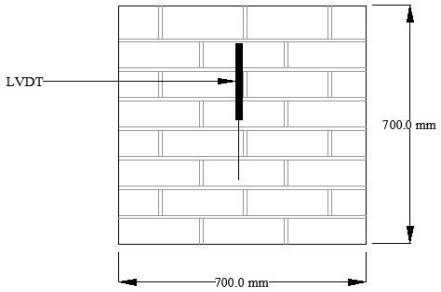

Figure 2 Dimensions and instrumentation of axial compression test

3. Experimental results

3.1 Tests on brick prisms

In this study, a total of 15 prism specimens using bricks were constructed i-e 2 bricks, 3 bricks, and 4 bricks masonry prisms were structured. The compressive strength of the prisms was investigated using UTM having capacity of 5000 KN in accordance with ASTM C1314-23a [14] after 28 days of curing. h/t ratio varied in the prism specimens i.e., 1.42 for 2 brick prisms, 2.17 for 3 brick prisms, and 2.93 for 4 brick prisms. The ultimate load, and the compressive strength of masonry prism specimens are shown in Table 3. It can be observed that the prism strength increases with the increase in the brick strength. The brick units possess the greater part of the prism's volume and provide a direct load transfer path. A similar variation was reported by Thaickavil and Thomas [19]. The variation of compressive strength of masonry prism with the influence of brick strength is shown in Fig.3.

Table 3 Results of test for axial compression on brick prisms

Sr. No.	Region	Single brick strength f_b (MPa)	Designation of prisms	h/t	Max. Load (kN)	Prism strength f_p (MPa)	Modulus of Elasticity E (MPa)
1	Zigzag		Z2	1.42	155	4.9	3675
2		13.9	Z3	2.17	115	4.4	3300
3			Z4	2.93	108.5	4.3	3225
4	Peshawar		P2	1.42	134.2	4.2	3150
5		11.3	P3	2.17	97	3.7	2775
6			P4	2.93	90.9	3.6	2700
7	Sargodha		S2	1.42	135	4.2	3150
8		9.8	S3	2.17	94.4	3.6	2700
9			S4	2.93	82.2	3.3	2475
10	Taxila		T2	1.42	103.5	3.2	2400
11		9.7	T3	2.17	75.9	2.9	2175
12			T4	2.93	69.5	2.8	2100
13	Quetta		Q2	1.42	93.5	2.9	2175
14		7.0	Q3	2.17	69.5	2.7	2025
15			Q4	2.93	50	2.0	1500

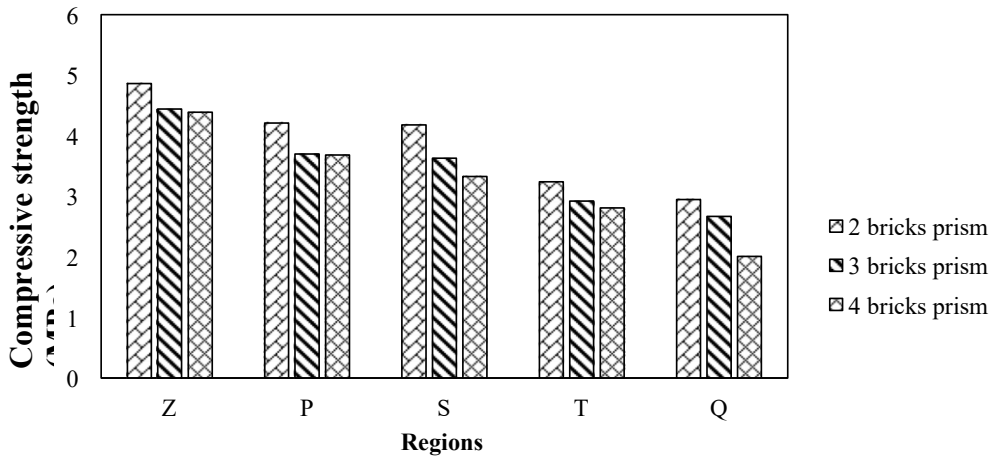

Figure 3 Influence of brick strength on the compressive strength of masonry prism

The percentages of water absorption of bricks are given in Table 2, the bricks collected from the Quetta region exhibited the highest absorption value of 19.9% as compared to other regions. Zig-zag kiln bricks showed the lowest absorption value of 12.96%. Absorption percentage has an inverse relation with the strength so that if the percentage absorption is higher than the compressive strength tends to decrease and vice versa [20,21] as shown in Fig. 3. Fig. 4 shows the comparison of the compressive strength of prisms of different regions with respect to the h/t ratio. The compressive strength of the prism decreases with an increase in the h/t ratio and bulge of specimens reflected Poisson's effect. However, due to the friction between the surface of the prism and steel plates of the machine, the top and bottom of the prism were restricted to bulge laterally and as a result of this, the middle zone of the prism was under tension and the top and bottom of the prism were under compression. A similar variation was reported by previous researchers [19] Masonry is weak in tension because of the weak links at the brick-mortar interface. When the height of the prism increases the zone subjected to tensile stress increases and this tensile zone is vulnerable to cracking due to which the strength of the prism decreased with the increase in height of the prism.

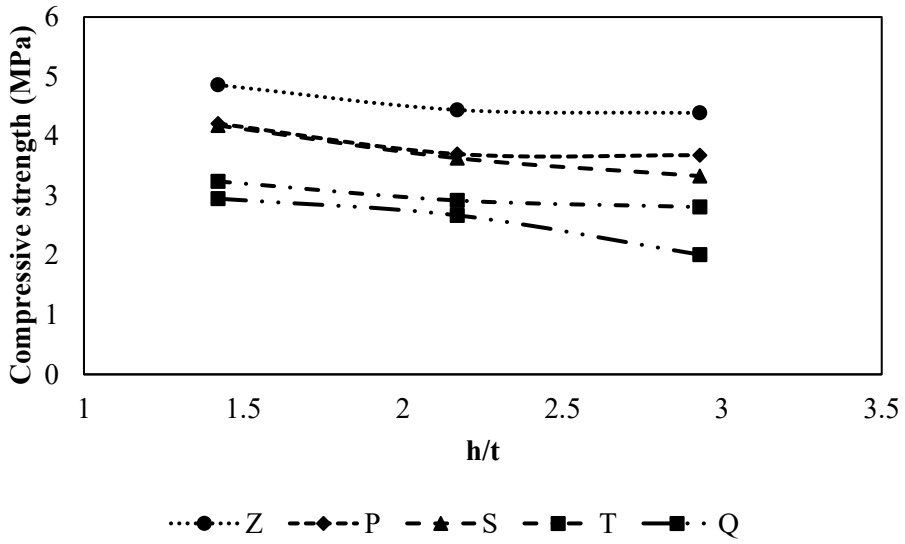

Figure 4 Effect of h/t ratio on the compressive strength of brick prisms

The failure pattern of brick prisms is shown in Fig. 5 where it can be seen that the failure occurred by vertical splitting. Under axial compression, bricks expand laterally but the soft brick strong mortar combination makes them confined hence, the mortar was subjected to a biaxial tension state and the bricks were subjected to a triaxial compression state, resulting in vertical splitting. A similar crack pattern was observed by previous researchers [22]. Teja [23] also investigated the mechanical properties of bricks and observed similar vertical splitting failure along with diagonal and crushing failure in the prism specimens.

Figure 5 Vertical splitting failure of brick prisms

3.2 Wall testing

3.2.1 Axial compression of the double brick wall

A total of ten wall specimens were constructed, one single brick wall and one double brick wall form each region were planned. The compressive strength results of double brmasonry wall specimens are shown in Table 4. The compressive strength of the wall specimens was calculated by dividing the ultimate load over the area of the wall. The Zig-zag brick wall failed at the ultimate load of 600 KN with an axial deformation of 2.8mm and a compressive strength of 3.7 MPa. The Zig-zag wall showed the highest ultimate load carrying capacity and compressive strength as compared to the other regions' walls. The Quetta region wall showed the lowest ultimate load carrying capacity of 374 KN with an axial deformation of 2.8 mm and its compressive strength was 2.34 MPa, which was also lowest as compared to the other regions' walls. The compressive strength of single brick affected the axial compressive strength of the wall as the strength of the Quetta region brick was lowest as compared to the other regions' bricks and ultimately its wall strength also turned

out to be the lowest in all the wall specimens. This could be attributed to the higher percent absorption of Quetta bricks. The failure in axial compression occurred by vertical cracking followed by splitting and crushing of bricks. This type of failure mainly occurs due to different strain characteristics of bricks and mortar joints. Vertical cracks occurred parallel to the direction of the applied load. It was investigated that masonry walls and small wallets in axial compression and concluded that the vertical cracks appeared first at the top course of bricks and then propagated all over the wall specimen.

Table 4 Axial compressive strength of double brick walls

Sr. No	Wall type	Ultimate load (kN)	Compressive strength (MPa)	Axial deformation (mm)
1	Z	600	3.7	2.8
2	P	523	3.3	2.2
3	S	430	2.7	3.4
4	T	400	2.6	1.7
5	Q	374	2.3	2.8

The graph in Fig. 6 illustrates the axial load versus axial deformation response of double brick masonry walls in the specified regions. Initially, all curves displayed linear behavior up to approximately 30% of the maximum load. This was attributed to connections between bricks and mortar, resulting in less cracks. However, as the load continued to increase, the bearing load capacity of the bricks diminished, leading to cracks in the mortar joints. The nonlinear behavior of the wall specimens was primarily associated with the initiation of vertical cracks. The combination of soft bricks and strong mortar caused the bricks to be confined, subjecting the mortar to a biaxial tension and the bricks to a triaxial compression, ultimately leading to vertical splitting failure. Notably, bricks from the Sargodha region exhibited confinement after reaching the ultimate load, indicating a higher load-bearing capacity. Smaller cracks were observed, and as the load increased, more cracks developed internally, showing a regular pattern of deformation.

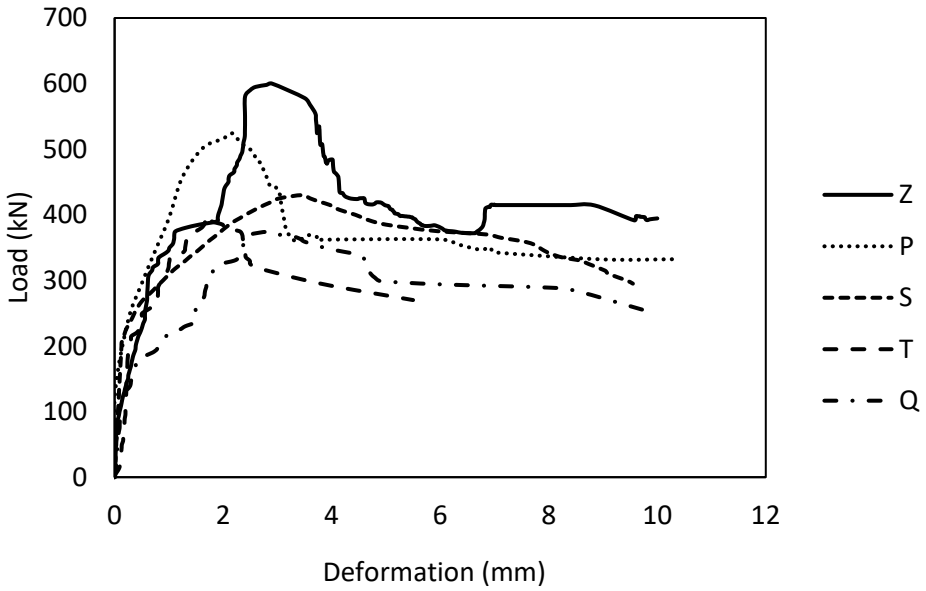

Figure 6 Axial load vs deformation of double brick walls

3.2.2 Axial compression of the single brick wall

The compressive strength results of single brick masonry wall specimens are shown in Table 5. The Zig-zag brick wall failed at the ultimate load of 290 kN with an axial deformation of 2.63 mm and a compressive strength of 3.62 MPa, which was highest compared to other wall types. The Quetta region wall showed the lowest ultimate load-carrying capacity of 180 kN with an axial deformation of 2.85mm and a compressive strength of 2.25 MPa, which was lowest as compared to other regions. The compressive strength of single bricks affected the strength of the wall as the Zig-zag bricks with the highest compressive strength as compared to other regions bricks also exhibited higher strength of Zig-zag brick wall. Tables 4 and 5 also demonstrate that the thickness of wall specimens affects the ultimate load-carrying capacity of the walls. The double brick walls exhibited higher load carrying capacity as compared to the single brick walls because of the lower slenderness ratio of the double brick wall. It has been indicated in the literature that as the slenderness ratio of masonry walls increases, the strength of the masonry wall decreases [24,25]. The slenderness ratio can be calculated by dividing the height over the thickness of the wall specimen. Kirtschig and Anstötz [26] also investigated the relationship between slenderness ratio and compressive strength and concluded that the strength of wall specimens decreased

by increasing the slenderness ratio. Similar to the double brick walls, vertical cracks occurred parallel to the direction of the applied load [27].

Table 5 Axial compressive strength of single brick walls

Sr. No	Wall type	Ultimate load (kN)	Compressive strength (MPa)	Axial deformation (mm)
1	Z	290	3.6	2.6
2	P	250	3.1	2.2
3	S	205	2.6	3.5
4	T	190	2.4	1.5
5	Q	180	2.2	2.8

The graphical representation in Fig. 7 illustrates the axial load versus axial deformation characteristics of single brick masonry walls. Similar trends were observed in single brick walls compared to their double bricks. Initially, all curves exhibited linear behavior up to approximately 30% of the maximum load, attributed to the limited development of cracks due to firm bonding between bricks and mortar. However, as the load increased, the bricks lost their load-bearing capacity, and cracks initiated in the mortar joints, leading to nonlinear behavior beyond the ultimate load. In wall specimens, the nonlinear behavior primarily resulted from the initiation of vertical cracks. The combination of bricks and mortar created a state of triaxial compression for the bricks and biaxial tension for the mortar. Notably, the Sargodha region brick exhibited significantly better post-ultimate load behavior, reflecting the similarity of performance observed in double brick walls. On the other hand, the Taxila region brick wall displayed more brittle behavior compared to other specimens, as of its lowest ultimate deformation.

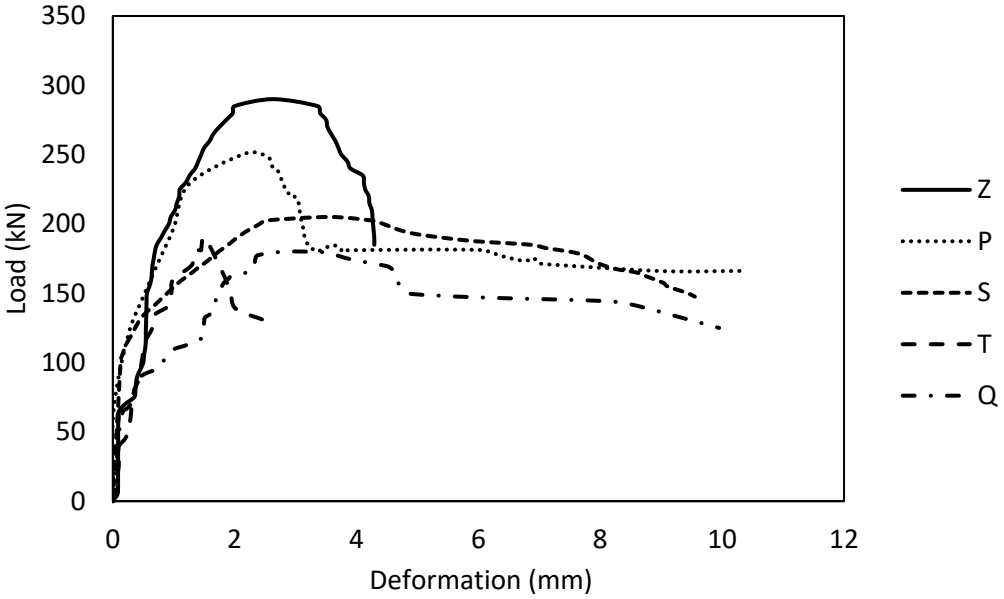

Figure 7 Axial load vs deformation of single brick walls

3.2.3 Ductility ratio of the wall specimens

The ductility level defines the capacity of the specimens to absorb energy and their ability to deform. Ductility is the ability of a structure or its members to undergo a wide inelastic deformation beyond the initial yield deformation without losing load-carrying capacity or without breaking before failure. A structure must have strength as well as ductility for adequate performance. Structures with adequate ductility will not collapse suddenly and can undergo large deformations and provide adequate time to evacuate before failure [28,29]. The ductility (μ) of the wall specimens was calculated as the ratio of ultimate deformation (Δu) to yield deformation (Δy), as shown in equation (1).

$$\text{Ductility} = \frac{\Delta u}{\Delta y} \quad (1)$$

The yield strain was calculated as 80% of the strength [30]. The ductility of double and single brick wall specimens is given in Tables 6 and 7, respectively. The Sargodha region brick wall showed the highest ductility as compared to other regions. More ductile behavior of the specimens reflects that they will absorb more energy before the collapse

[31]. The Quetta region brick showed the lowest ductility as compared to other regions. The ductility of both single and double brick wall specimens was in good agreement with the standard requirement which specifies that the minimum ductility ratio for unreinforced masonry walls should be at least 1.25. The ductility ratio of double and single brick wall specimens of different regions is presented in Figs. 8 and 9, respectively. The ductility factor is affected by the stiffness of the wall specimens as stiffer structure exhibits more brittle behavior.

Table 6 Ductility of double brick wall specimens subjected to axial compression

Sr. No	Wall type	Δu (mm)	Δy (mm)	μ
1	Z	2.80	0.69	4.1
2	P	2.10	0.75	2.8
3	S	3.40	0.71	4.8
4	T	1.71	0.69	2.5
5	Q	2.81	1.51	1.9

Table 7 Ductility of single brick wall specimens subjected to axial compression

Sr. No	Wall type	Δu (mm)	Δy (mm)	μ
1	Z	2.60	0.72	3.6
2	P	2.21	0.75	2.9
3	S	3.50	0.47	7.4
4	T	1.51	0.65	2.6
5	Q	2.81	1.31	2.1

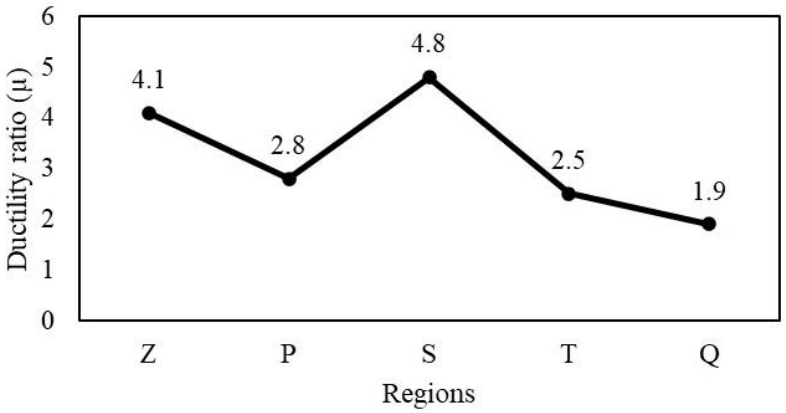

Figure 8 Ductility ratio of double brick walls

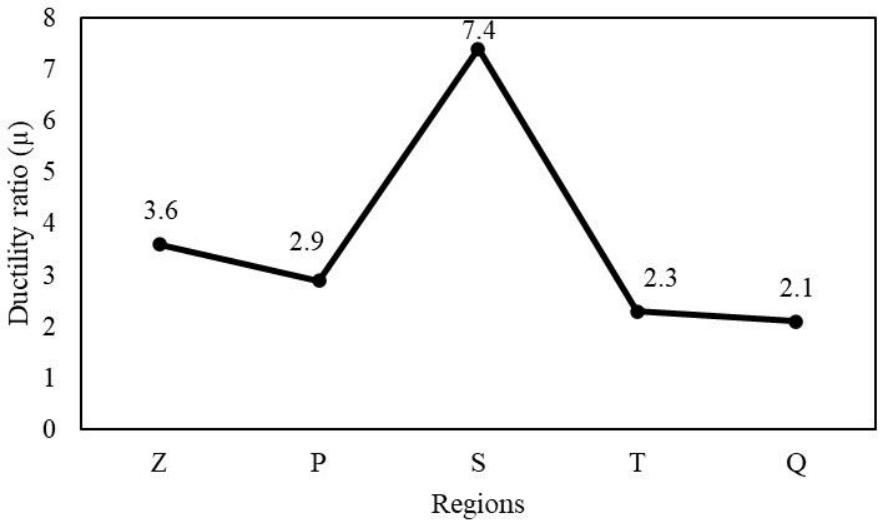

Figure 9 Ductility ratio of single brick walls

3.2.4 Application of DIC technique for axial deformation

An analytical technique of 2D digital image correlation was also used to correlate the deformations results. Digital image correlation (DIC) is an optical technique that incorporates image registration and tracking methods for precise 2D measurements of changes in images [32,33]. In 1975, correlation theories for measuring data changes were extended to digital images for the first-time digital image correlation is a very effective technique to measure deformations and strains without employing LVDTs or a data logger [34]. A digital camera of 18MP with a frequency of 30Hz was used to obtain high-quality images of the test specimens

correlate software that was used as an easily accessible opensource platform. For DIC analysis, the creation of the stochastic pattern is a crucial step [35]. High contrast images are required to optimize the DIC analysis. For this purpose, the specimens were painted with white paint, and different points were marked on the front face and a black speckled pattern was applied on the back face of the wall for strains, as shown in Fig 10. The videos of the whole test were recorded at the rate of 30 frames per second to obtain high-quality images. The timeline of the videos recorded by the digital camera was then synchronized with the time recorded by the data logger. A facet of 30x30 pixels was used to track the deformation of the wall during the test. The results obtained from the two-dimensional image correlation (GOM) and LVDTs were compared.

(a) Back side (b) Front face

Figure 10 Black speckle pattern over the face of the wall

3.2.5 Comparison of axial deformation of double and single brick walls with DIC technique

Load deformation curves for the double brick wall specimens of each region, as obtained by the experimental and DIC technique, are shown in Fig. 11. The agreement was found to be reasonably good between the LVDT and DIC measurements. The percentage difference between the experimental and DIC values of maximum deformations for Zigzag, Peshawar, Sargodha, Taxila, and Quetta regions was 3.57%, 0.46%, 1.62%, 1.16%, and 1.79%, respectively. The percentage difference between the experimental and DIC values of maximum deformations for double brick walls of Zigzag, Peshawar, Sargodha, Taxila, and Quetta regions was 2.63%, 0.92%, 1.3%, 1.99%, and 1.05%, respectively.

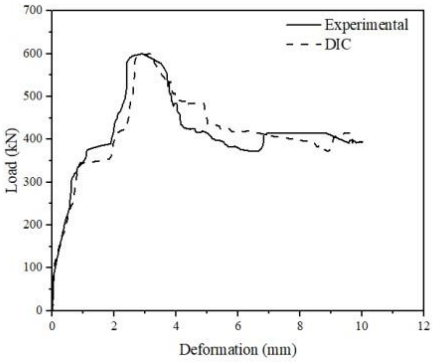

(a) Zigzag

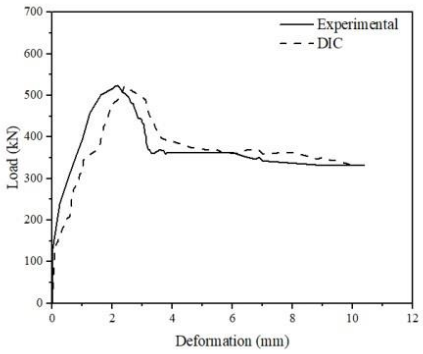

(b) Peshawar

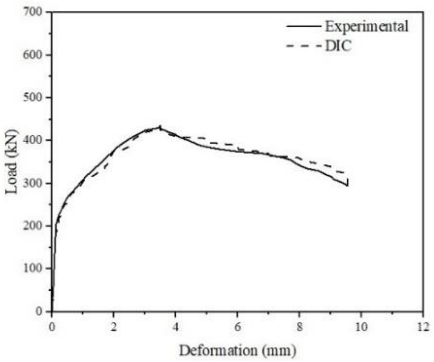

(c) Sargodha

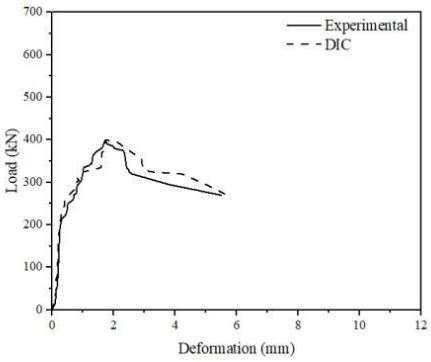

(d) Taxila

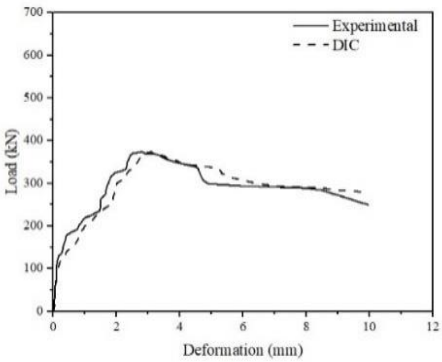

(e) Quetta

Figure 11 Comparison of experimental and DIC calculated axial deformations of double brick wall specimens

Table 8 Comparison of Axial Deformation of Walls with DIC and FEM

Sr. No	Wall type	% Difference b/w experimental and DIC values (Single brick)	% Difference b/w experimental and DIC values (Double brick)	% Difference b/w experimental and FEM values (Single brick)	% Difference b/w experimental and FEM values (Double brick)
1	Z	3.75	2.63	0.76	3.1
2	P	0.46	0.92	19.72	0.46
3	S	1.62	1.3	6.94	1.27
4	T	1.16	1.99	0.66	1.16
5	Q	1.79	1.05	0.35	2.14

3.3 Failure modes of the wall specimens

The observed failure patterns are similar, primarily with significant damage at both the upper and lower courses of the wall. In the case of axial compression on the wall specimens, the primary mode of failure was the development of vertical (flexure) cracks aligning parallel to the applied load direction. Subsequent failures ensued as a result of the splitting and crushing of the bricks within the loading region. In addition to these principal cracks, numerous minor cracks manifested on the walls. The damage initiation originated from the brick surface and extended across the wall surface through joints. The level of brick damage was high due to the comparatively higher compressive strength of the mortar.

Lenczner [36] described the brick-and-mortar behavior subjected to axial load and concluded that the mortar joint appears to expand laterally when the load is applied because of its less rigid behavior, as compared to bricks. When the tensile stress on a brick surpasses its ultimate tensile strength, failure occurs. In our case, the combination of a weak brick and strong mortar resulted in the mortar experiencing tension, while the brick underwent compression. The failure of the brickwork under axial compression primarily initiated from vertical splitting caused by distinct strain characteristics in both mortar joints and bricks. Additionally, horizontal tension in the bricks contributed to the overall failure. Similar behavior was also observed.

Fig. 12 and 13 show the same crack pattern in both the experimental and DIC technique. Cracks observed by DIC showed a good relationship with the experimental results [37].

(a) Double brick wall (b) Single brick wall

Figure 12 Failure modes of wall specimens subjected to axial loading.

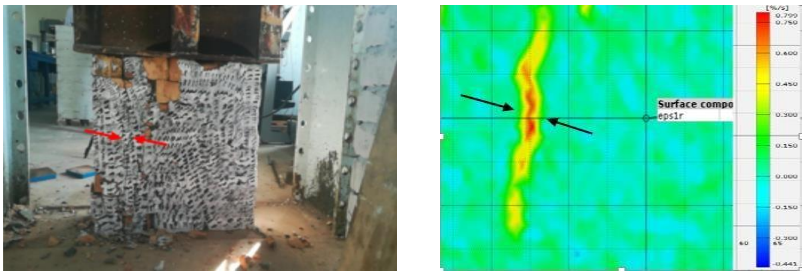

(a) (b)

Figure 13 Crack pattern (a) experimental view (b) DIC crack visibility

3.4 Finite element modeling of brick walls

For the numerical idealization of the actual member, accuracy in the modelling of element type and size, geometry, material properties, boundary conditions, and loads is essential. Finite element modeling was carried out to compare experimental and analytical results. Abaqus software was used for numerical modeling of brick masonry walls under axial compression [38]. There are several ways to model masonry in Finite Element Analysis (FEA) varying from a very detailed micro-level to a composite macro level, as discussed by Van Noort [39] and Lourenço [40]. The macroscale model was used in this study. For modeling masonry walls, two parts were defined in the “Part Module” of Abaqus, i.e., top beam, and the masonry wall. These parts were created as 3d deformable type with a solid shape as recommended by previous studies [41,42]. The parts were meshed in the “Mesh Module” of Abaqus but before that, an approximate global seed size of 70 mm was provided from the menu bar in part. The model geometry of a simple and meshed wall is shown in Fig. 14. For both Abaqus/Standard and Abaqus/Explicit, the “Concrete Damaged Plasticity model” was applied, offering a general capability for concrete analysis and appropriate for

masonry. The masonry wall was connected to the beam by forming a surface-to-surface contact in the create [43,44].

(a) (b)

Figure 14 Model geometry used in Abaqus (a) simple wall (b) meshed wall

"Interaction Module". A reference point (RP-1) was made on the girder to connect it to the wall and load was applied as shown in Fig. 15. Based on previous research the displacement type boundary condition was applied at the top part and ENCASTRE boundary condition was applied to the wall's bottom.

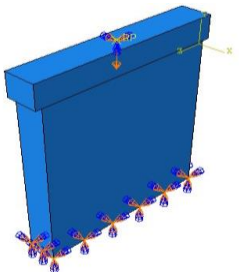

Figure 15 Model showing boundary conditions and load applied in axial compression testing

3.4.1 Comparison of axial compression behavior of double and single brick walls using Abaqus

Abaqus software was used to analytically determine the axial compressive behavior of the wall specimens. The percentage difference between the experimental and analytical values of maximum deformation of double brick wall for Zigzag, Peshawar, Sargodha, Taxila, and Quetta regions' bricks was 3.1%, 0.46%, 1.27%, 1.16%, and 2.14%, respectively. The percentage difference between the experimental and analytical values of maximum load for

the above-mentioned region's bricks was 0.33%, 1.23%, 0.47%, 0.25%, and 0.27%, respectively. Load deformation curves for the single brick wall specimens of each region are shown in Fig. 16. The percentage difference between the experimental and analytical values of maximum deformation for Zigzag, Peshawar, Sargodha, Taxila, and Quetta regions, bricks was 0.76%, 19.72%, 6.94%, 0.66%, and 0.35%, respectively. The percentage difference between the experimental and analytical values of maximum load for the above-mentioned regions bricks was 0.34%, 0.8%, 2.93%, 1.58%, and 3.78%, respectively. A good agreement between the experimental and Abaqus results was observed for both single and double brick walls. Fig.17 (a-d) shows the comparison of damage visualization of the wall specimens using Abaqus. It can be observed that the compression starts from the top of the wall and propagates all over the specimen. The failure of the brickwork under axial compression is usually attributed to horizontal strain in the bricks due to vertical splitting [36]. After observing the crack pattern in software at different stress levels, it was observed that initially, the cracks developed on the upper side of the wall below the girder and then propagated all over the wall.

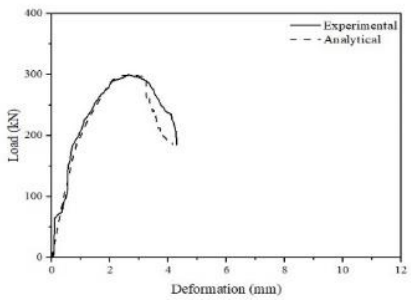

(a) Zigzag

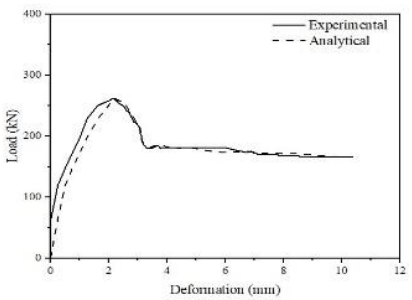

(b) Peshawar

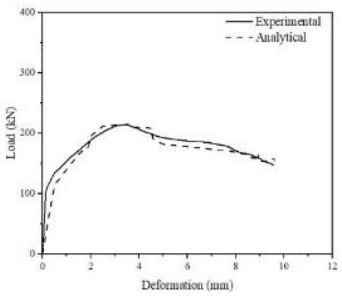

(c) Sargodha

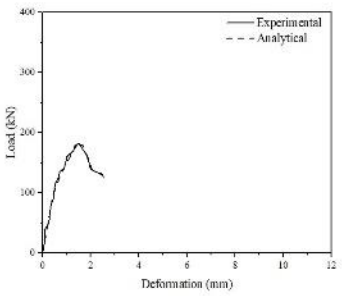

(d) Taxila

Figure 16 Comparison of the experimental and analytical deformation of single brick wall specimens subjected to axial compression.

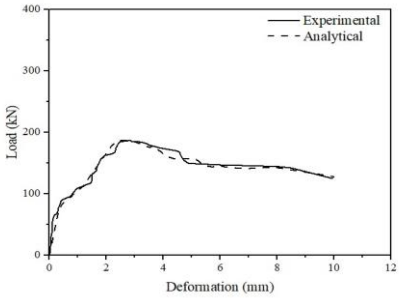

(e) Quetta

Figure 16 (continued) Comparison of the experimental and analytical deformation of single brick wall specimens subjected to axial compression

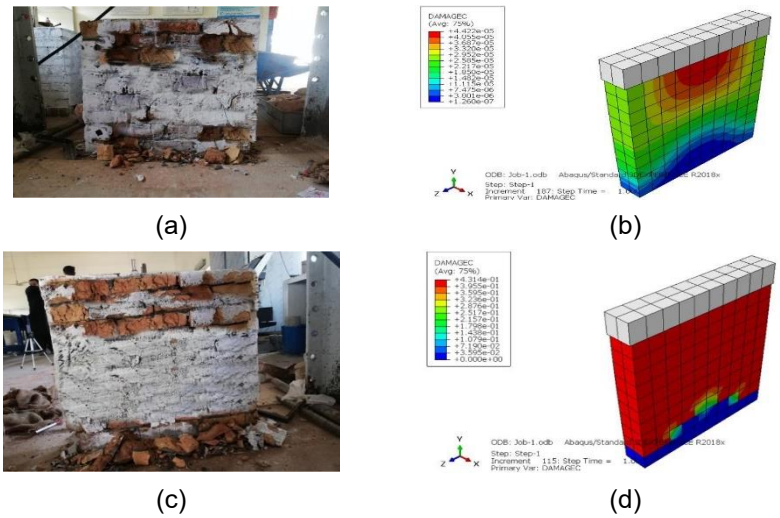

(a) (b)

(c) (d)

Figure 17 Comparison of damage visualization using Abaqus (a), (c) Experimental view (b), (d) Abaqus software view

4. Conclusion

Masonry walls using different types of bricks are tested against uniaxial compression. The results of deformations and strains as well as a digital image correlation are concluded as follows.

Bricks from the Peshawar region demonstrated superior mechanical properties among conventional kilns, while zig-zag kiln bricks outperformed their conventional counterparts. However, prisms constructed with zig-zag kiln bricks exhibited higher compressive strength

than those from other regions. The study revealed that single brick strength directly influenced masonry prism strength, which decreased with higher h/t ratios. zig-zag kiln bricks also resulted in enhanced compressive strength in both single and double brick walls compared to bricks from other regions.

Validation using LVDT values confirmed the accuracy of deformations obtained through digital image correlation (DIC), indicating satisfactory results. Additionally, DIC monitoring proved effective in identifying incipient cracks before visible signs emerged. This cost-effective DIC system presents a viable alternative for full-scale structural testing, offering potential improvements over existing monitoring approaches. The analytical results obtained by Abaqus software were in good agreement with the experimental results.

Acknowledgment

The authors are very grateful to the Higher Education Commission of Pakistan (HEC) for providing the research grant to carry out this research work.

References

[1] Sutcu M, Alptekin H, Erdogmus E, Er Y, Gencel O. Characteristics of fired clay bricks with waste marble powder addition as building materials. Construction and Building Materials 2015;82:1-8.

[2] Climate & Clean Air Coalition secretariat. Pakistan moves toward environmentally friendly and cost-effective brick kilns. Paris: United Nations Environment Programme; 2018.

[3] Zhang L. Production of bricks from waste materials – a review. Construction and Building Materials 2013;47:643-55.

[4] Oti JE, Kinuthia JM, Robinson RB. The development of unfired clay building material using Brick Dust Waste and Mercia mudstone clay. Applied Clay Science 2014;102:148-54.

[5] Toure PM, Sambou V, Faye M, Thiam A. Mechanical and thermal characterization of stabilized earth bricks. Energy Procedia 2017;139:676-81.

[6] Dondi M, Marsigli M, Venturi I. Microstructure and mechanical properties of clay bricks: comparison between fast firing and traditional firing. British Ceramic Transactions. 1999;98(1):12-8.

[7] Singh SB, Munjal P. Bond strength and compressive stress-strain characteristics of brick masonry. Journal of Building Engineering 2017;9:10-6.

[8] Chen Z, Chen W, Mai C, Shi J, Xie Y, Hu H. Experimental study on the compressive behaviors of brick masonry strengthened with modified oyster shell ash mortar. Buildings 2021;11(7):266.

[9] Joyklad P, Hussain Q. Experimental study on axial and diagonal compressive behavior of brick masonry walls. Kasem Bundit Engineering Journal 2018;8(2):1-20.

[10] Lalchandani D, Maithel S. Towards cleaner brick kilns in India: a win-win approach based on zigzag firing technology. Dehli, India: Greentech Knowledge Solutions; 2013.

[11] The Express Tribune. Brick kiln innovation: zig-zag technology can cut pollution. The Express Tribune. 2018 Sep 13.

[12] Yooprasertchai E, Saingam P, Hussain Q, Khan K, Ejaz A, Suparp S. Development of stress-strain models for glass fiber reinforced polymer composites confined sustainable concrete made with natural and recycled aggregates. Construction and Building Materials 2024;416:135097.

[13] Ali K, Saingam P, Qureshi MI, Saleem S, Nawaz A, Mehmood T, et al. Influence of recycled plastic incorporation as coarse aggregates on concrete properties. Sustainability 2023;15(7):5937.

[14] ASTM International. ASTM C1314-23a. Standard test method for compressive strength of masonry prisms. West Conshohocken (PA): ASTM International; 2023.

[15] ASTM International. ASTM C1717-18. Standard test methods for conducting strength tests of masonry wall panels. West Conshohocken (PA): ASTM International; 2018.

[16] ASTM International. ASTM C67-17. Standard test methods for sampling and testing brick and structural clay tile. West Conshohocken (PA): ASTM International; 2017.

[17] ASTM International. ASTM C1006-07. Standard test method for splitting tensile strength of masonry units. West Conshohocken (PA): ASTM International; 2007.

[18] ASTM International. ASTM C109/C109M-16a. Standard test method for compressive strength of hydraulic cement mortars (Using 2-in. or [50-mm] cube specimens). West Conshohocken (PA): ASTM International; 2013.

[19] Thaickavil NN, Thomas J. Behaviour and strength assessment of masonry prisms. Case Studies in Construction Materials 2018;8:23-38.

[20] Deboucha S, Hashim R. Correlation between total water absorption and wet compressive strength of compressed stabilised peat bricks. International Journal of the Physical Sciences 2011;6(10):2432-8.

[21] Ali N, Mohd Yusup NF, Sheikh Khalid F, Shahidan S, Abdullah SR. The effect of water cement ratio on cement brick containing High Density Polyethylene (HDPE) as sand replacement. MATEC Web of Conferences 2018;150:03010.

[22] Sathiparan N, Rumeshkumar U. Effect of moisture condition on mechanical behavior of low strength brick masonry. Journal of Building Engineering 2018;17:23-31.

[23] Teja PRR. Studies on Mechanical Properties of Brick Masonry [thesis]. Rourkela : National Institute of Technology Rourkela; 2015.

[24] Hasan SS, Hendry A. Effect of slenderness and eccentricity on the compressive strength of walls. In: Proceedings of the 4th International Brick Masonry Conference; 1976 Apr 26-28; Brugge, Belgium.

[25] Wan Ibrahim WR. Effect of the slenderness ratio on masonry wall under axial compressive cyclic loading [dissertation]. Penang, Malaysia: Universiti Sains Malaysia; 2014.

[26] Kirtschig K, Anstötz W. Kinckuntersuchungen an mauerwerksproben. In: Proceedings of the 9th International Brick/Block Masonry Conference; 1991 Oct 13-16; Berlin, German. p. 202-9.

[27] Churilov S. Experimental and analytical research of strengthened masonry [dissertation]. Skopje, Macedonia: University Ss. Cyril and Methodius; 2012.

[28] Paulay T, Priestley MN. Seismic design of reinforced concrete and masonry buildings. New York: John Wiley & Sons; 1992.

[29] Faizah R, Satyarno I, Priyosulistyo H, Aminullah A. Improving the masonry brick ductility using mortar bed joint from rubber tire crumbs: a review. Journal of Physical Science 2018;29 Suppl 2:117-32.

[30] Mahmood H, Ingham J. Diagonal compression testing of FRP-retrofitted unreinforced clay brick masonry wallettes. Journal of Composites for Construction 2011;15:810-20.

[31] Triwiyono A, Nugroho ASB, Firstyadi AD, Ottama F. Flexural strength and ductility of concrete brick masonry wall strengthened using steel reinforcement. Procedia Engineering 2015;125:940-7.

[32] Gu J, Liu G, Yang Q, Law SS. Improved SURF method in digital image correlation for estimation of large rotation angle. Measurement 2023;207:112372.

[33] Mudassar AA, Butt S. Improved Digital Image Correlation method. Optics and Lasers in Engineering. 2016;87:156-67.

[34] Keating TJ, Wolf PR, Scarpace FL. An improved method of digital image correlation. Photogrammetric Engineering and Remote Sensing 1975;41(8):993-1002.

[35] Strauss A, Castillo P, Bergmeister K, Krug B, Wan-Wendner R, Marcon M, et al. Shear performance mechanism description using digital image correlation. Structural Engineering International. 2018;28(3):338-46.

[36] Lenczner D. Elements of loadbearing brickwork. Oxford: Pergamon Press; 1972.

[37] Chen Y, Yan Q, Jia B, Yu X, Wu Y, Luo Y. Experimental and mechanical behavior of rubber-sleeved group studs. KSCE Journal of Civil Engineering 2022;26(9):3905-17.

[38] Dassault Systèmes. Abaqus analysis user's guide. Proidence (RI), USA: Dassault Systèmes Simulia Corp, 2014.

[39] Van Noort JR. Computational modelling of masonry structures [thesis]. Delft, Netherlands: Delft University of Technology; 2012.

[40] Lourenço PB. Computational strategies for masonry structures [Ph.D. thesis]. Delft, Netherlands: Delft University of Technology; 1996.

[41] Rafiq A. Computational modelling of unconfined/unreinforced masonry wall using Abaqus [thesis]. Peshawar, Pakistan: University of Engineering and Technology; 2016.

[42] Rehman F, Khan SA, Ur Rehman S, Khan MS, Saleem U, Mughal S, et al. Finite element analysis of brick masonry. In: Proceeding of 2nd Pak-Turk International Conference on Emerging Technologies in the field of Sciences and Engineering; 2019 Mar 11-12; Swabii, Pakistan.

[43] AlGohi BH, Baluch MH, Rahman MK, Al-Gadhib AH, Demir C. Plastic-damage modeling of unreinforced masonry walls (URM) subject to lateral loading. Arabian Journal for Science and Engineering 2017;42(9):4201-20.

[44] da Silva LCM, Milani G, Lourenço PB. Probabilistic-based discrete model for the seismic fragility assessment of masonry structures. Structures 2023;52:506-23.

Author's Profile

Muhammad Zohaib Asim, Lecturer at Civil Engineering Department, University of Technology, Islamabad, Pakistan. Concrete Lab, Ground Flour, Civil Engineering Department, NUTECH. +92 336 5745371, muhammad.zohaib@nutech.edu.pk, Masters in Structural Engineering, Structural Materials

Dr Adnan Nawaz, Associate Professor at Civil Engineering Department, COMSATS University Wah Campus, Pakistan, Civil Engineering Department, CUI Wah, +92 51 9314382, adnannawaz@ciitwah.edu.pk, PhD in Structural Engineering, Structural Materials

Dr Tahir Mehmood, Associate Professor at Civil Engineering Department, COMSATS University Wah Campus, Pakistan, Civil Engineering Department, CUI Wah, +92 51 9314382, tahirmemood@ciitwah.edu.pk, PhD in Structural Engineering, Structural Materials.

Ali Siddique, Lecturer at Civil Engineering Department, University of Technology, Islamabad, Pakistan. Fifth Flour, Civil Engineering Department, NUTECH. +92 340 3226679, ali.saddique@nutech.edu.pk, Masters in Structural Engineering, Structural Materials.

Sajid Rasheed, Lecturer at Civil Engineering Department, University of Technology, Islamabad, Pakistan. Fifth Flour, Civil Engineering Department, NUTECH. +92 301 7588295, sajidrasheed@nutech.edu.pk, Masters in Structural Engineering, Structural Materials.

Asim Sultan, Lecturer at Civil Engineering Department, University of Technology, Islamabad, Pakistan. Fifth Flour, Civil Engineering Department, NUTECH. +92 331 8148045, asim.sultan@nutech.edu.pk, Masters in Structural Engineering, Structural Materials.

Article History:

Received: September 17, 2024

Revised: July 22, 2025

Accepted: August 1, 2025